Wavelet Transform Based Denoising in Transient Evoked OAE Measurement

Han-Chang Wu [*,1] Shuenn-Tsong Young [2] Te-Son Kuo [1,3]

[1] *Department of Electrical Engineering, National Taiwan University, Taipei, Taiwan, 106, ROC*
[2] *Institute of Biomedical Engineering, National Yang-Ming University, Taipei, Taiwan, 112, ROC*
[3] *Graduate Institute of Biomedical Engineering, National Taiwan University, Taipei, Taiwan, 106, ROC*

Received 19 October 2002; Accepted 13 November 2002

Abstract

The major purpose of this paper is to investigate the theories of various time-frequency analysis (TFA) and its capabilities in representing TEOAE signals. Owing to the tiny, noisy and nonstationary characteristics of TEOAE signals, conventional time- and frequency- domain based analysis are not adequate to extract all the information embedded within the original signals. TFAs can effectively decompose the original signals into time-frequency distributions (TFDs) that can provide both time and frequency resolutions. More precise medical diagnosis can thus be achieved. Because TFAs can represent signal features more efficiently, higher performance is accomplished in several biomedical applications, such as signal compressions, and pattern recognitions, by TFA-based signal processing methodologies. The mathematical backgrounds of several commonly used linear and quadratic TFAs are described. We used a simulated TEOAE signal to testify that the TFAs can efficiently decompose the original signal, and the results of various TFAs are compared and discussed. The specific feature of how different frequency components vary with time, which is similar to the Cochlear organ, can be successfully extracted by the wavelet transform. Because the acquired TEOAE signals are severely contaminated by environmental white noise, we designed a TFA-based active denoising methodology, called wavelet shrinkage, to suppress the embedded white noise during the measurement. The proposed method is more efficient than traditional statistically averaging method and is implemented in the DSP-based system.

***Keywords*:** TEOAE, Wavelet Transform, TFA, Denoising

Introduction

Otoacoustic Emissions (OAEs) are acoustic signals emitted by the cochlea. It reflects the active processes that are involved in the transduction of mechanical energy into electrical energy [1]. One of the most attractive features is the tight relation between OAEs and the cochlear status. The OAEs are universally present to a various degree in all healthy cochlear, whereas they are generally missed or are greatly reduced in the ears with mild and severe hearing losses. This aspect, together with the extreme facility of test performance and with the high reproducibility both on short-term and on long-term progression, has made the OAEs as an increasingly widespread neonatal hearing screening method [2]. Due to their good long-term reproducibility, OAEs can also be used to monitor the cochlear functionality in patients exposed to prolonged noise or ototoxic agents [3][4]. Two typical OAEs are currently used for clinical applications. They are the transient-evoked OAEs (TEOAEs), and distortion-product OAEs (DPOAEs) [5]. The TEOAEs are delayed responses to acoustic-transient stimuli of short duration (about 80u~100us), and DPOAEs are inter-modulation-distortion responses to two simultaneous and pure-tone stimuli. The TEOAEs express the transient characteristics of the hearing system, while the DPOAEs show the static one.

The TEOAEs are nonstationary signals and exhibit clear frequency dispersion along with time. The time of appearance of a component seen in a TEOAE is intimately related to the frequency of the component itself, i.e. the higher the frequency the shorter the latency, and vice versa, the lower the frequency the longer the latency. Analysis of time-frequency properties of TEOAEs is therefore of considerable interest due to their close relation with cochlear mechanisms. It is hardly to extract the full information within the TEOAE by traditional time domain or frequency domain analysis. The traditional Fourier transform is not suitable for the description of transient signals (such as TEOAEs) since it gives no information on frequency changes along with time. During the past decades, the time frequency analyses (TFAs) have been shown to represent nonstationary signals more efficiently. In this chapter, TEOAE signals will be applied by several TFAs. A simulated TEOAE

* Corresponding author: Han-Chang Wu
Tel: +886-2-83693611; Fax: +886-2-83693612
E-mail: peterwu@ecareme.com

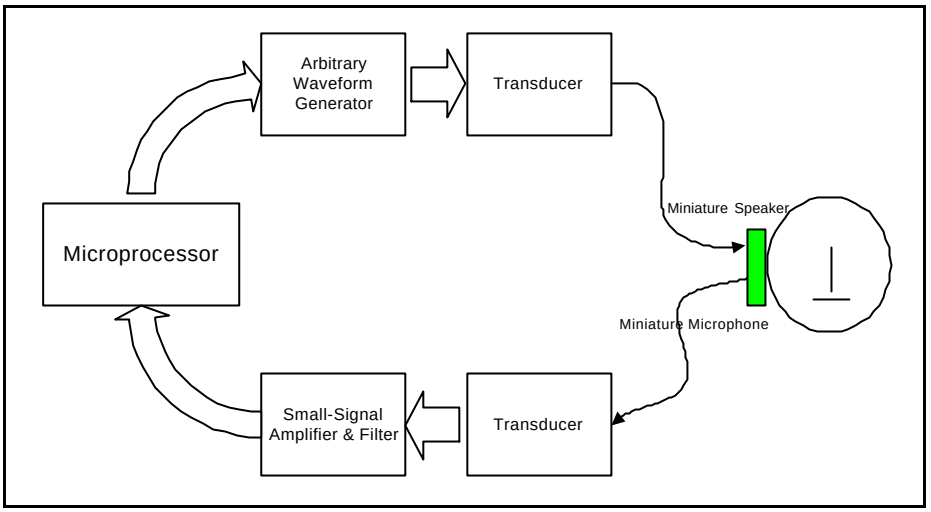

Figure 1: Functional block diagram of OAE measurement.

will be conducted first to evaluate the effectiveness of the TFAs, and the real TEOAEs will be investigated.

Besides the nonstationary feature, the measurement of TEOAEs is not easy because of its tiny and noisy characteristics [6]. As illustrated in figure 1, the TEOAEs are stimulated and monitored by miniature microphones, and are then conditioned by high-gain amplifiers and filters. The measured TEOAEs are easily contaminated by artificial noise and environmental noise. The artificial noise originated from the stimulus-induced ringing and can be suppressed by nonlinear differential method. The environmental noise is modeled by white noise and is suppressed by conventional signal-averaging method and statistically decreased by $\sqrt{N}$ after N responses. Although the signal-averaging method is undoubted useful, it prolongs the measurement time. In typical clinical trials, a TEOAE signal needs 1,024 stimuli, and this equates to 42 seconds if no samples are rejected because of unwanted noise contamination during the measurement. A TFA-based denoising methodology, called wavelet shrinkage, will be introduced to suppress the white noise more efficiently.

Materials and Methods

Mathematical background of time-frequency analyses

The time-frequency distributions of signals are conventionally classified into two categories: linear distribution and quadratic distribution. The linear time-frequency distribution satisfies the linearity superposition principle, while the quadratic (or energetic) time-frequency distribution satisfies the quadratic superposition principle. The quadratic distribution exhibits two types of signal terms: the auto-terms (the true time-frequency distribution of each signal component) and cross-terms (the interference artifacts). For any time-frequency distribution, there is a trade-off between time resolution and frequency resolution. The time resolution and the frequency resolution could not be arbitrarily good that is proved by the uncertainty principle [7]:

$$\Delta t \cdot \Delta f \geq 1/4p \tag{1}$$

where Δt and Δf represent the standard deviation (or resolution) of time and frequency distribution of a signal.

In many time-frequency analyses, analytic signals are chosen because of their better instant frequency and group delay explanation. In the study, analytic simulated signals are then used, and real, physiological signals ($x(t)$) are also transformed into analytic signals $(x_a(t))$ by Hilbert transform $H(f)$:

$$x_{a(t)} = x(t) + j \cdot H(x(t)) \tag{2}$$

The short-time Fourier transform (STFT)

STFT is a linear time-frequency distribution defined as

$$STFT_x^{(w)}(t',w) = \int [x(t) \cdot w^*(t-t')] \cdot e^{-2wt}\, dt \tag{3}$$

where $w(t)$ is the sliding analysis window and * denotes the complex conjugation. The time and frequency resolutions depend on the length and on the bandwidth of $w^*(t)$. Once the analysis window $w^*(t)$ is chosen and kept same for all the analysis frequencies, the time and frequency resolutions are fixed on the time-frequency plane. Therefore, the analysis window dominantly determines the properties of the STFT. The more detail definitions are discussed in the literature [8].

The energetic version of STFT is the spectrogram (SPEC) defined as the squared magnitude of the STFT

$$SPEC(t',w) = \left| STFT_x^{(w)}(t',w) \right|^2 \tag{4}$$

Certain interferences also exhibit in the spectrogram as oscillatory structure, but they occur only if there is overlap between the transforms of auto-terms.

The wavelet transform

The WT is also a linear distrubution defined as:

$$WT_x^y(t,s) = \Psi_{t,s} = \int \frac{1}{\sqrt{s}} x(t) y\left(\frac{t-t}{s}\right) dt \quad (5)$$

The WT can be described as a time-scale distribution because its properties are determined by a scale factor s, where s = f_o / f. Like the STFT, the WT is also a product of original signal $x(t)$ and a window function $y(t)$, namely the wavelet or sometimes called mother wavelet. However, as the definition, the mother wavelet is scaled by s and shifted by t over the time-frequency plane, so the obtained time and frequency resolutions are not fixed.

The energetic version of the WT is the scalogram (SCALO) defined as the squared magnitude of the WT

$$SCALO(t,s) = \left| WT_x^y(t,s) \right|^2. \quad (6)$$

The scalogram is a quadratic distribution. Its interference terms are restricted to the area of the time-frequency plane where the time-frequency distributions of the auto-terms are overlapped.

The Wigner-Ville distribution

The WVD is a quadratic distribution defined as

$$WVD(t,w) = \int x\left(t+\frac{t}{2}\right) \cdot x^*\left(t-\frac{t}{2}\right) \cdot e^{-jwt}\, dt \quad (7)$$

The WVD has a very high time-frequency concentration [9], whereas SPEC and SCALO introduce some broadening with respect to time and frequency. The major drawback of the WD is the presence of cross-terms. In the WVD, cross terms have oscillations of relatively high frequencies and may have a peak value as high as twice that of the auto-term. For example, the WVD of the sum of two signals $x_1(t) + x_2(t)$ is

$$WVD_{x_1+x_2}(t,w) = WVD_{x_1}(t,w) + 2\,\mathrm{Re}[WVD_{x_1,x_2}(t,w)] + WVD_{x_2}(t,w) \quad (8)$$

The cross-term interferences become more severe when the there are more signals appeared. By the 2-D Fourier transform of the WVD, the desired information will be concentrated in low frequency parts, i.e. the center of the image, and the cross-terms will reside in the high frequency parts. The cross-term interferences can be attenuated by means of a smoothing which is a sort of two-dimension low-pass filtering. The smoothing is achieved by convolving the WVD with a kernel $j(t,t)$

$$SWVD(t,w) = \int j(t-t',t) \cdot x\left(t'+\frac{t}{2}\right) \cdot x^*\left(t'-\frac{t}{2}\right) dt' \cdot e^{-jwt}\, dt \quad (9)$$

After low-pass filtering of the WVD by certain smoothing kernels, the cross-term interferences can be decreased. However, the smoothing kernels also result in a loss of time-frequency concentration; that means the resolution decrease. There then exhibits a trade-off between interference levels and the time-frequency resolution. The most common smoothed WVD are the following.

a. The smoothed pseudo WVD (SPWVD) [10] for which

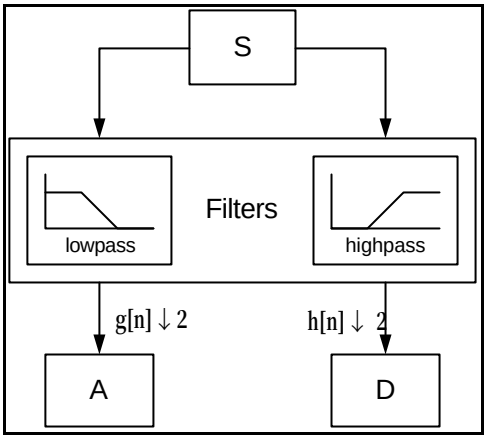

Figure 2: The Mallat 's method to decompose the original signals by filter banks.

$j(t,t) = g(t) \cdot h\left(\frac{t}{2}\right) \cdot h^*\left(\frac{t}{2}\right)$. The smoothing along the time-frequency direction is determined by the length of the windows $g(t)$ and $h(t)$.

b. The Choi-Williams distribution (CWD) [11], or exponential distribution (ED) for which $j(t,t) = \sqrt{\frac{s}{4p}} \bullet \frac{1}{|t|} \bullet e^{-s\left(\frac{t}{2t}\right)^2}$. The smoothing is controlled by the parameter s ($s > 0$). A good compromise between time-frequency resolution and interference attenuation can be obtained for $0.1 \le s \le 10$.

The DWT and inverse DWT

In section 2.1, the TFAs are introduced as appropriate methods to represent nonstationary signals, especially for noninvasive physiological signals. Besides providing better interpretation of the signals, the TFAs also provide good basis for signal processing. With the capability of transforming signals into time-frequency decompositions, time-frequency based signal processing can provide advanced performance than traditional time- or frequency-based signal processing methodology. However, the conventional algorithms for computing TFAs is huge and is not possible for real-time signal processing. Therefore, fast algorithms for real-time processing are thus necessary for noninvasive instrumentation.

The linear TFAs, such as the STFT and WT, are preferred in real-time signal processing because they are much easier to handle than quadratic TFAs. The STFT can be treated as a series of windowed FFT, so the computation complexity is $N \log(N)$, which is feasible for the DSP-based system. Although the WT can represent the physiological signals more efficiently than the STFT, the computation complexity of the WT is N^2 and is also not suitable for real-time signal processing. However, as the Fourier transform uses orthogonal signals to represent the original signal, we can also acquire more concise TFAs by orthogonal wavelets. The orthogonal WT, also called the DWT, can be achieved by dyadic-shifted and translated wavelets as defined below:

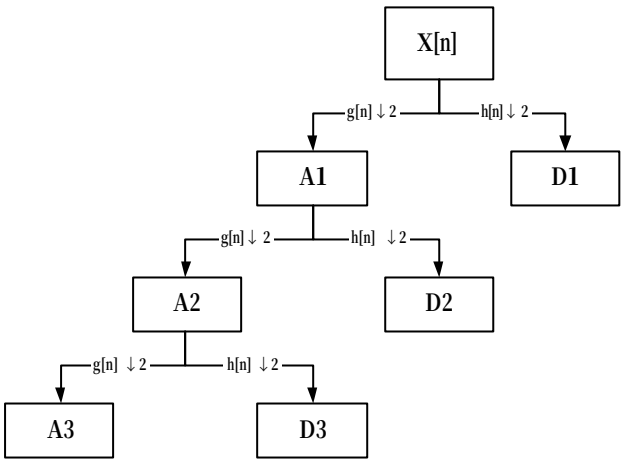

Figure 3: The cascaded wavelet decomposition of filter banks and decimations.

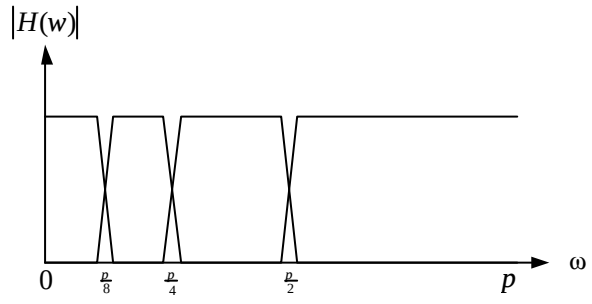

Figure 4: Spectrum of the high-pass filters in each segment.

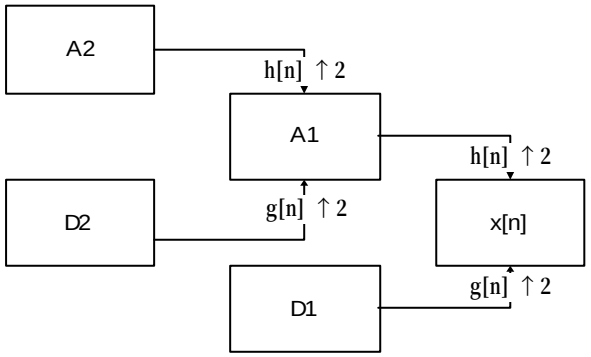

Figure 5: Signal reconstruction by cascaded filter banks and interpolations.

$$OWT_x^y(j,k) = \Psi_{j,k} = \int \frac{1}{\sqrt{a}} x(t) y\left(\frac{t-b}{a}\right) dt, \qquad (10)$$

where $a = 2^j, b = ka, j,k \in Z$.

Mallat proposed a more efficient way to compute the DWT by using filter banks. Different from computing the convolution of the dyadic wavelets and the original signal, Mallat applied a high-pass filter and a low-pass filter to the original signal, and then decimated the filtered signals by two, as illustrated in figure 2. The resulted signals after applying the high-pass filter and the low-pass filter are called the detail coefficients and approximation coefficients, respectively. It can be proved that the DWT can be achieved by cascaded filter banks, as shown in figure 3. The wavelet coefficients of the DWT can be represented by the detail coefficients of each level. The frequency response high-pass filters in the different cascaded filter banks can be illustrated in figure 4. The first level high-pass filter has the widest frequency spectrum ($p/2 \sim p$), and the second high-pass filter occupies another half of the remaining spectrum ($p/4 \sim p/2$). The higher the level is approaching, the narrower frequency spectrum and fewer detail coefficients are accomplished, i.e., when higher frequency resolution is used, lower time resolution is inevitable. We can also reconstruct the original signal perfectly by using the cascaded filter banks by replacing the decimation operator by a interpolating operation, as shown in figure 5, thus the inverse DWT (IDWT) is also accomplished.

The translation-invariant DWT (TIDWT)

In the DWT computation, the decimation operator is utilized with the filter banks to obtain orthogonal wavelet coefficients. But the decimation operator results in different results as the phase of the original signal changes, or translates. Therefore, the DWT is a translation-variant transformation and may cause serious problems in some applications. In the compression of nonstationary, wide-band transients, such as ECG compression, the performance of DWT-based compression algorithms may deteriorate when the signals not aligned in time properly. In pattern recognition applications, such as EMG recognition, when we try to match two signals from their wavelet coefficients, it is very desirable that the representation be insensitive to phase shifts. In the denoising applications, as we will discussed in chapter 4, the phase shifts may result in severe artifacts. The TIDWT is a methodology to compute a set of wavelet coefficients that is insensitive to phase shifts. Mallat proposed an algorithm to represent a signal from its wavelet coefficients, which is invariant to time shifts [12]. The algorithm first calculates the decomposition of the signal in the various levels without the decimation. The coefficients are then averaged by n different phase-shifted signals. The resulted wavelet coefficients are thus time-invariant

Wavelet transform based denoising

The environmental white noise is suppressed statistically by averaging a lot of TEOAE samples. Nevertheless, the white noise can be also decreased by the TFA-based wavelet shrinkage method. Because TEOAEs can be represented by localized time-frequency components, we can separate the signals and white noise into time-frequency domains. In normal samples, the power of time-frequency coefficients of TEOAEs should be much larger than those of the spreading white noise. After applying thresholding algorithms, the noise below certain thresholds can be eliminated and only the signals will be remained. Therefore, the reconstructed TEOAEs will be noise-free. The active method usually shows great efficiency than the signal-averaging method. Donoho proposed this wavelet shrinkage denoising method [13]. Many researches also showed that Donoho's methods could enhance many biomedical signals and images without losing high-frequency information [14][15].

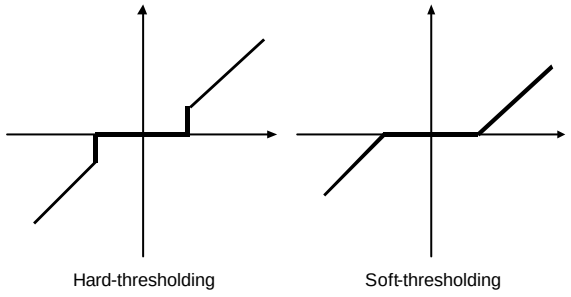

Figure 6: Hard and soft thresholding transfer functions.

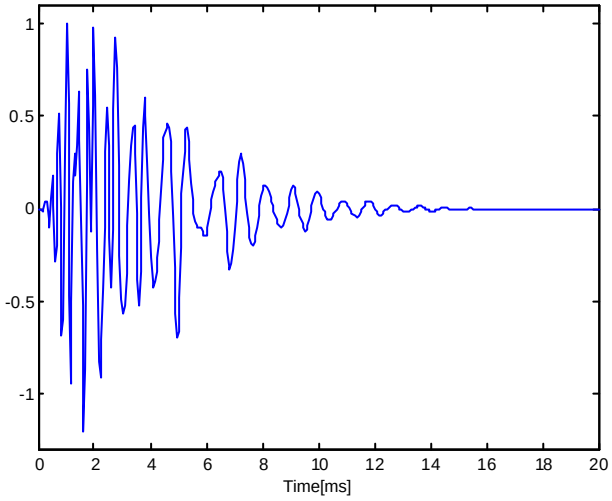

Figure 7: Simulated TEOAE signal by five gammatones

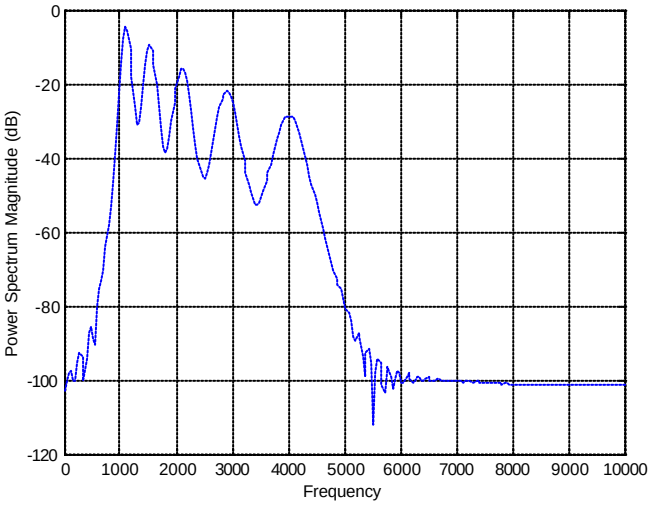

Figure 8: Power spectrum density of the simulated TEOAE signal.

Donoho's wavelet shrinkage method can be summarized by four steps: 1) applying a linear forward wavelet transform, 2) estimating the noise level 3) applying a nonlinear shrinkage denoising, and 4) applying a linear inverse wavelet transform. Compared to traditional filtering method, after applying a high-pass filter, not only the noise is suppressed, high-frequency signals will also be eliminated. This is not feasible in biomedical applications because the high-frequency signals usually carry a lot of useful information. There are two kinds of nonlinear shrinkage functions, soft-thresholding and hard-thresholding, and their transfer functions are illustrated in figure 6. The hard-thresholding function set the signal to zero if they are below a certain threshold, and the soft-thresholding simply cut the entire signal into two parts by the threshold. In general, the hard-thresholding function has better SNR than that of the soft-thresholding function, but the latter has better visually smoothed effect on the signal.

Simulated TEOAE signals

TEOAEs can be simulated by the summation of a series gammatones $g_i(t)$ [16]

$$s(t) = \sum_{i=1}^{N} g_i(t) \tag{11}$$

where $g_i(t) = a \cdot t^3 \cdot e^{-2\pi b f_i t} \cdot \cos(2\pi f_i t)$, $a = (2\pi f_i)^{3.5}$, b is a constant and f_i is the central frequency of the i th gammatone. We chose f_i =1.1kHz, 1.53kHz, 2.10kHz, 2.90kHz and 4kHz, sampled at 20kHz with 20ms of duration, and the resulted time-domain signal and frequency domain signal are shown in figure 7 and figure 8, respectively. As we can see, the high-frequency component has short latency, while the low-frequency component has long latency.

Results and Discussions

TFAs of the TEOAE signals

Figure 9 illustrates the TFDs of simulated TEOAEs. The SCALO after apply the WT shows great decomposition of the gammatones. Each gammatone can be extracted precisely. High-frequency component has good time resolution and low-frequency component has good frequency resolution. Compared to the power spectrum density in the frequency domain, where each gammatone is only identified by the frequency value, the SCALO is more similar to the cochlear mechanism. The SPEC after applying the STFT can also show the frequency dispersion along with time. However, it has poor discrimination because of the fixed time and frequency resolution in the entire time-frequency plain. The WVD provides extremely high time-frequency resolution, but severe interferences contaminate the auto-terms. The reduced interference distributions, both the CWD and the SPWVD, have low interferences under the tradeoffs of frequency resolution. Among the TFDs, the SCALO and CWD can achieve good signal decomposition, and the SCALO has no interferences. Therefore, the WT shows as a suitable TFA for TEOAE signal processing.

A Real TEOAE from a normal adult is shown in figure 10 (a). The SCALO and CWD of the signal are also demonstrated in figure 10 (b) (c). In the SCALO, various frequency components with different latencies are discriminated. There exist a 3.8KHz component with 4ms latency, a 2.6KHz component with 5.8ms latency, and a 2KHz component with 6.3ms latency. We can also identify these components in the

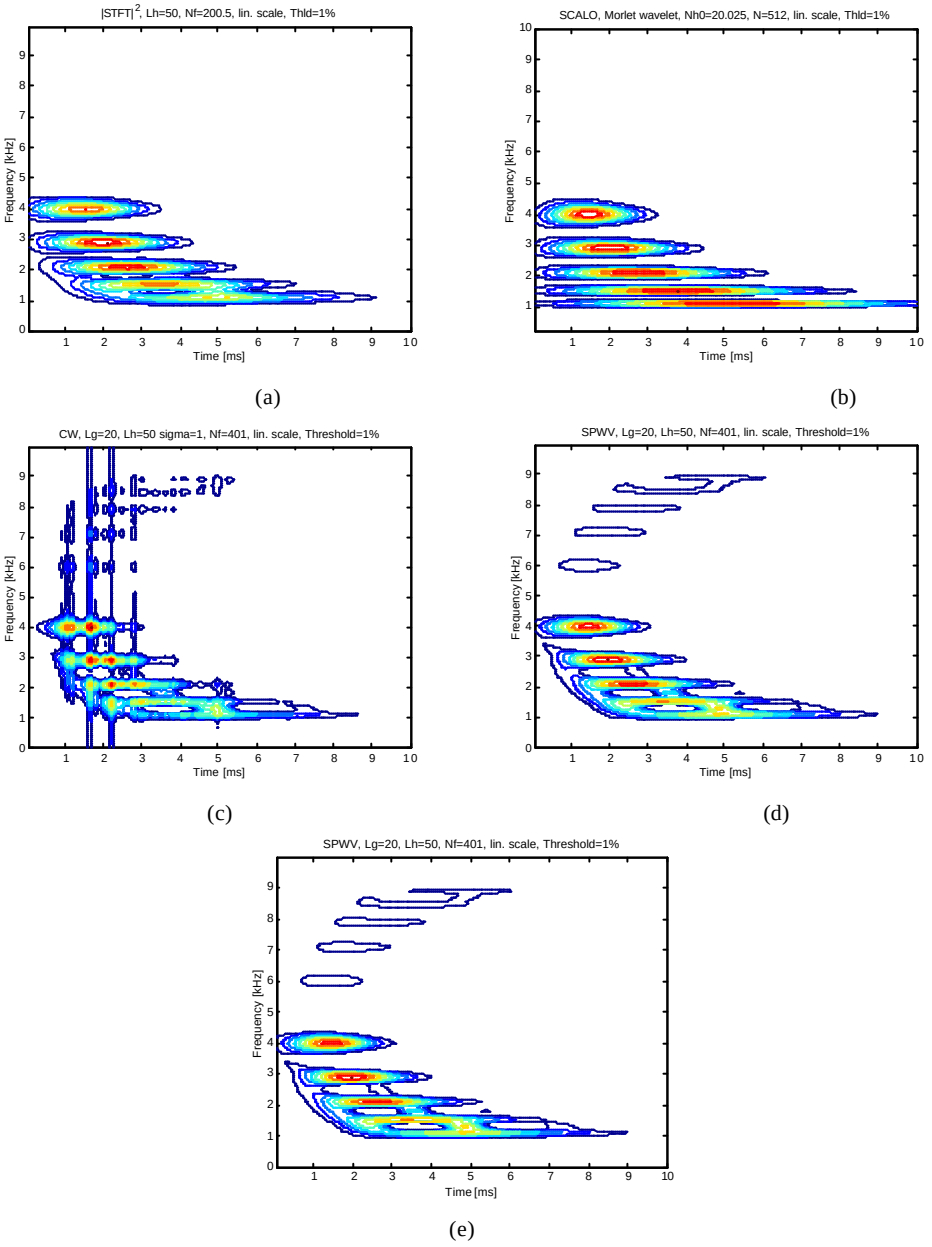

Figure 9: Time-frequency distributions of the simulated TEOAE signal. (a) SPEC (b) SCALO(c) WVD (d) CWD(e) SPWVD

CWD, and its time-frequency resolution is higher than the SCALO. There also shows interferences in the CWD. Another real TEOAE measured from a normal neonate and its TFDs are presented in figure 11. There also shows some differences in the TFDs between the adult and the neonate. The latencies of the normal neonate are shorter than those of the normal adult. The high-frequency components in the adult TEOAE decay faster than those in the neonate Moreover, most of the components in the neonate TEOAE scatter in higher frequency planes. We can hardly see the distributions below 1KHz. However, there are some components at around 500Hz in the TFDs of the adult TEOAE.

Wavelet transform based denoising

Figure 12 shows the results after applying the wavelet shrinkage method to a noisy simulated TEOAE signal (SNR=9.8dB). The original wavelet coefficients are presented in (b). The embedded information is dispersed into different scales. In the high-frequency scale, the high-frequency component with low latency is extracted. As the scale goes to low frequency, the original TEOAE signal is successfully decomposed into an orthogonal plane. As shown in (d), the wavelet coefficients of the white noise scatter in every scale with the same amplitude. After applying the soft-thresholding function with an estimated threshold, the noisy coefficients are eliminated. The denoised signal is then reconstructed by the IDWT, and resulted SNR is 11.60dB. Although the noise is suppressed, the soft-thresholding function also shrinks by the threshold and the SNR is thus not high. We chose a five-scale

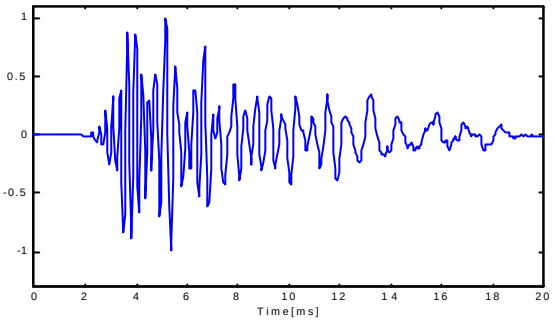

(a)

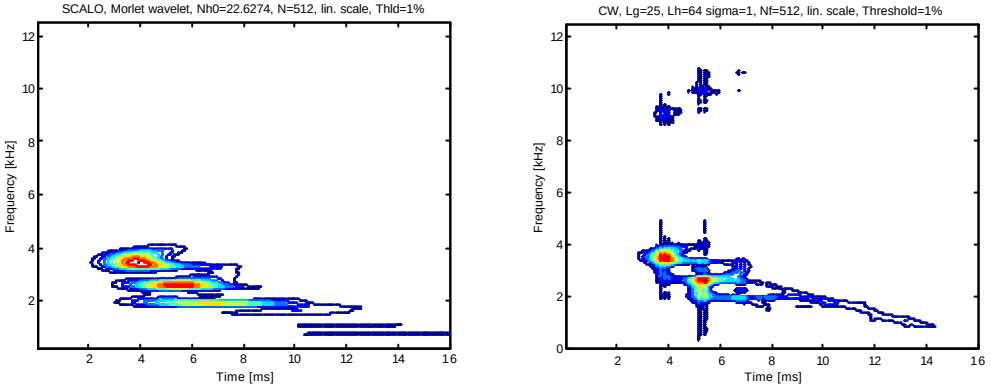

(b) (c)

Figure 10: A real TEOAE signal of a normal adult and its time-frequency distributions. (a) time domain representations(b) SCALO (c) CWD

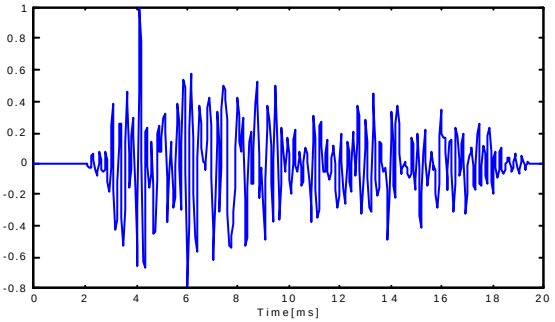

(a)

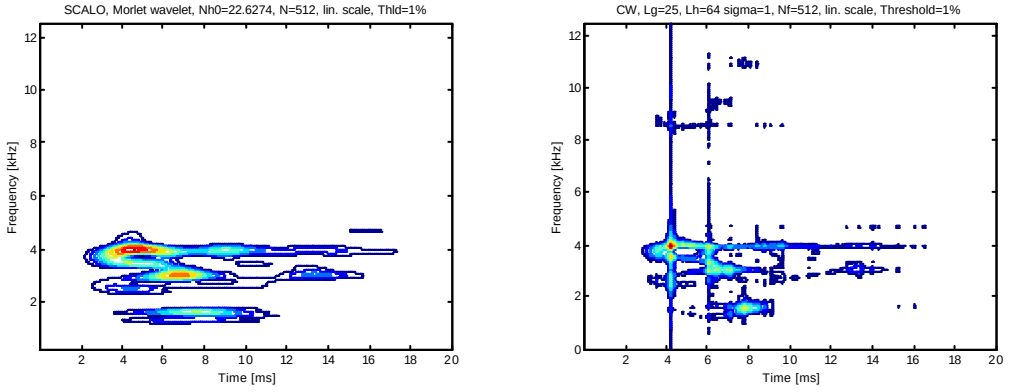

(b) (c)

Figure 11: A real TEOAE signal of a normal neonate and its time-frequency distributions. (a) time domain representations(b) SCALO (c) CWD

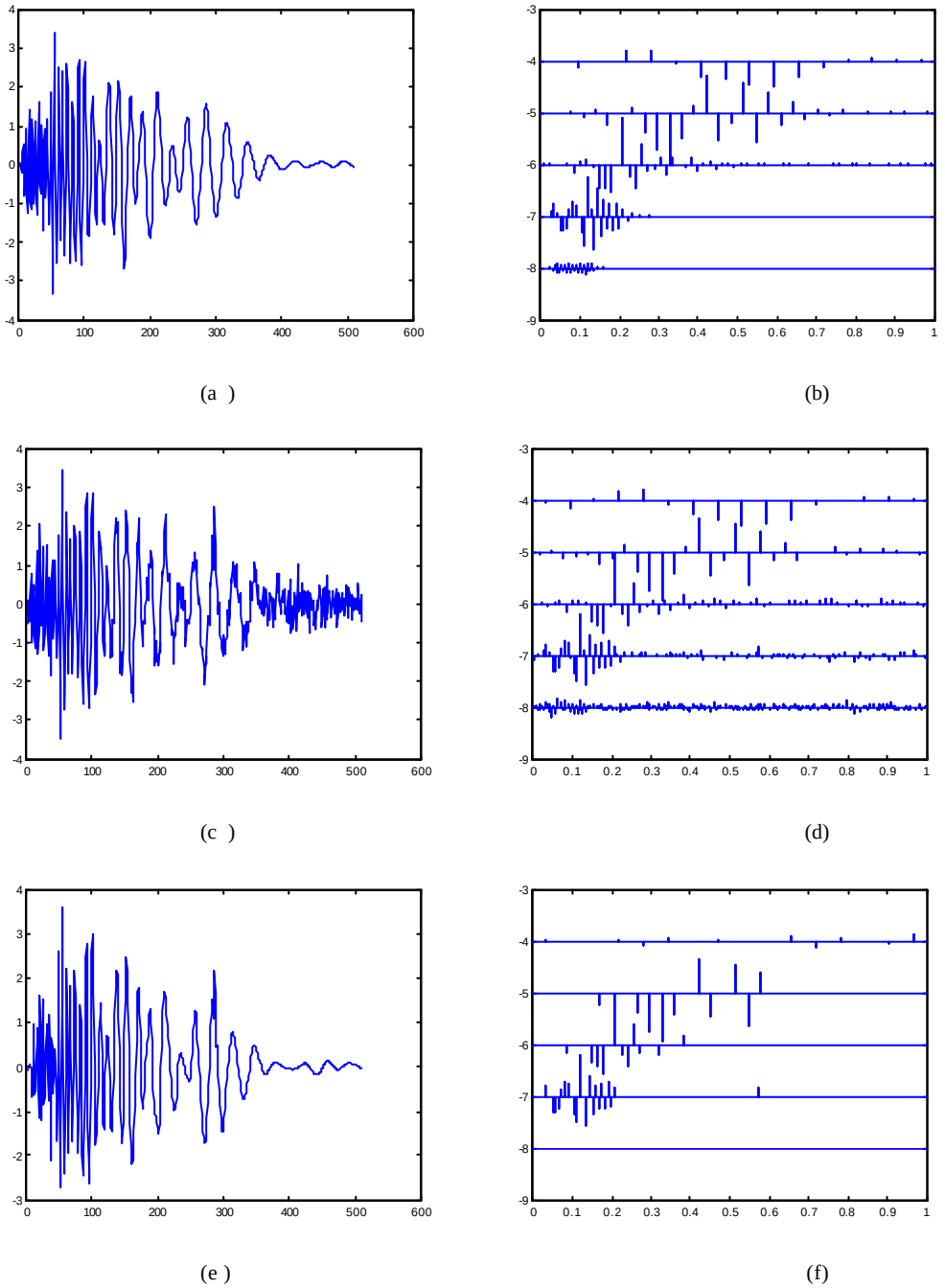

Figure 12. Wavelet shrinkage denoising on the simulated TEOAE signal. (a)original signal (b) original wavelet coefficients (c)noisy signal (d) noisy wavelet coefficients(e) reconstructed signal after denoising (f) wavelet coefficients after thresholding

DWT and IDWT and the Daubechies wavelets. Both the DWT and IDWT are implemented by cascaded filter banks.

In figure 12 (e), we can also observe that there are some glitches in the reconstructed signal. The glitches stem from the decimation of the DWT, as we introduced in 2.3. The problem can be solved by the TIDWT. The reconstructed TEOAE signal by the TIDWT is shown in figure 13. The glitches are eliminated in both the hard-shrinkage (SNR=14.46dB) and the soft-shrinkage functions (SNR=9.6415dB).

The SNR of reconstructed TEOAEs are compared based on the original signals with different SNRs, different decomposition methods, and different selection of mother wavelets, as illustrated in figure 14. It can be observed that the active denoising will enhance the SNR by 2~6dB for either severe noisy signals (SNR=0dB) or normal noisy signals (SNR=20dB). The SNR of reconstructed TEOAEs by the classical DWT is always poorer than by the TIDWT. Furthermore, the effects of the mother wavelets are complicated. The Coiflet wavelet and Symmlet wavelet provide better SNR results than other wavelets.

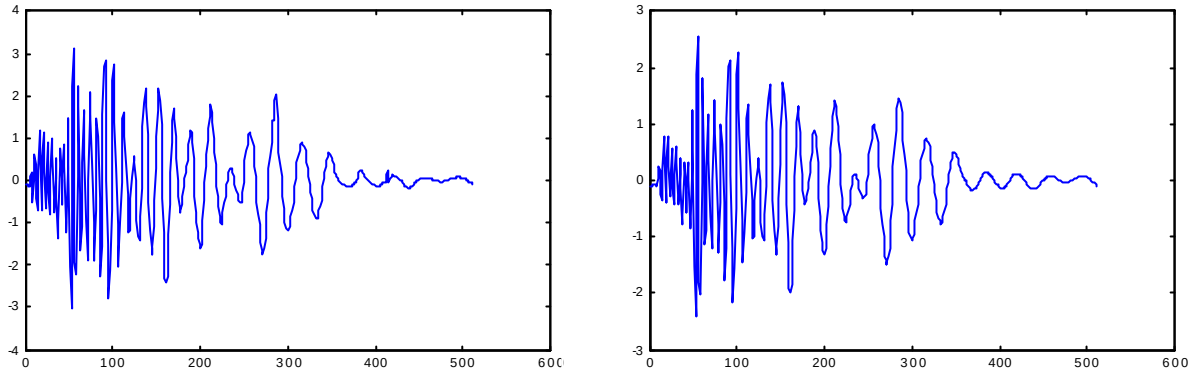

(a) (b)

Figure 13: Wavelet shrinkage denoising by translation-invariant DWT. (a) by using hard-thresholding, (b) by using soft-thresholding

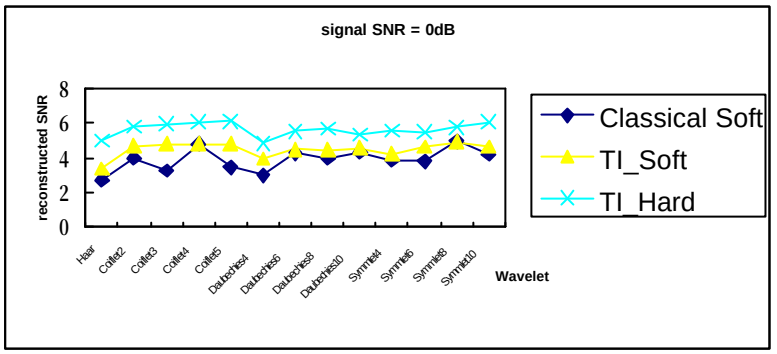

(a)

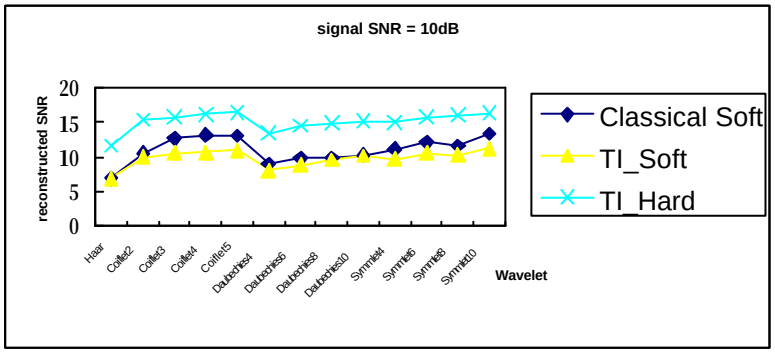

(b)

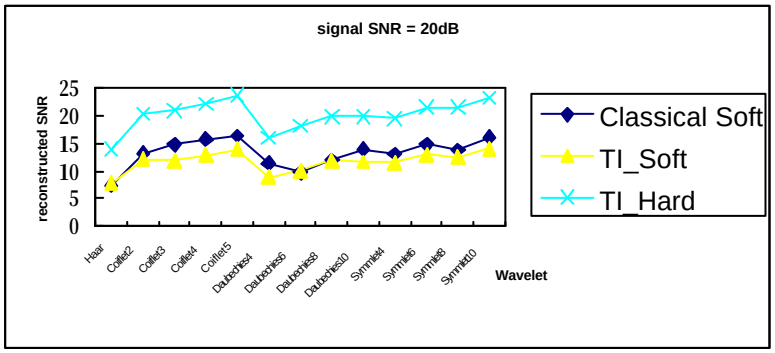

(c)

Figure 14: SNR of reconstructed signal after wavelet shrinkage denoising. (a) original SNR = 0dB (b) original SNR = 10dB (c) original SNR 20dB

Conclusions

In the research of OAE measurement, a DSP-based instrument is developed for OAE monitoring, and the transient-evoked OAE signals are of considerable interests. We used a simulated TEOAE signal to testify that the TFAs can efficiently decompose the original signal, and the results of various TFAs are compared and discussed. The specific feature of how different frequency components vary with time, which is similar to the Cochlear organ, can be successfully extracted by the wavelet transform. Because the acquired TEOAE signals are severely contaminated by environmental white noise, we propose a TFA-based active denoising methodology, called wavelet shrinkage, to suppress the embedded white noise during the measurement. The proposed method is more efficient than traditional statistically averaged signals and is implemented in the DSP-based system.

References

[1] D.T. Kemp, "Evidence of mechanical nonlinearity and frequency selective wave amplification in the cochlea", *Arch. Otolaryngol*,. 224: 37-45, 1979.

[2] S.J. Norton, "Application of transient evoked otoacoustic emissions to pediatric populations", Ear Hearing, 14: 64-73, 1993.

[3] R. Rubsamen, D.M. Mills, and E.W Rubel, "Effects of furosemide on distortion product otoacoustic emissions and on neuronal responses in the anteroventral cochlear nucleus", *J. Neirophysiol.*, 74:1628-1638, 1995.

[4] B. Engdahl and D.T. Kemp, "The effect of noise exposure on the details of distortion product otoacoustic emissions in humans", *J. Acoust. Soc. Amer.*, 99: 573-1587, 1996.

[5] R. Probst, "A review of otoacoustic emissions", *J. Acoust. Soc. Amer.*, 89: 2027-2067, 1991.

[6] M. L. Whitehead, B. B. Stagner, B. L. Lonsbury-Martin, and G.. K. Martin, "Measurement of otoacoustic emissions for hearing assessment", *IEEE Engineering in Medicine and Biology*, 210-226, 1994.

[7] L. Cohen, "Time-frequency analysis", New Jersey, Prentice hall, 1995.

[8] F. J. Harris, "On the use of windows for harmonic analysis with the discrete Fourier transform," *Proc. IEEE*, 66: 51-83, 1978.

[9] D. L. Jones and T. W. Parks, "A resolution comparison of several time-frequecny representations", *IEEE trans. Signal Processing*, col. 40: 413-420, 1992.

[10] W. Martin and P. Flandrin, "Wigner Ville spectral analysis of nonstationary processes", *IEEE Trans. Acoust., Speech, Signal Processing*, ASSP-33: 1461-1470, 1985.

[11] H. I. Choi and W. J. Williams, "Improved time-frequency representation of multicomponent signals using exponential kernels", *IEEE Trans. Acoust. Speech, Signal Processing*, 37: 862-871, 1989.

[12] S. Mallat, "Zero-crossings of a wavelet transform", *IEEE Trans. Information Theory*, 37: 1019-1033, July 1991.

[13] D. L. Donoho, "De-Noising by Soft-thresholding", *IEEE. Trans. Information Theory*, 41(3): 613-627, 1995.

[14] P. Carre, H. Leman, C. Fernandez, and C. Marque, "Denoising of the uterine EHG by an undecimated wavelet transform", *IEEE Trans. Biomedical Engineering*, 45(9):1104-1113, 1998.

[15] A. Aldroubi and M. Unser, "Wavelets in medicine and biology", CRC Press, 1996.

[16] G. Tognola, D. Grandori, P. Ravazzani, "Time-frequency distributions of click-evoked otoacoustic emissions", *Hearing Research*, 106: 112-122, 1997.